EXERGY EFFICIENCY AND EXERGY DESTRUCTION CHANGE OF LOW POWER STEAM TURBINE WITH ONE CURTIS STAGE DURING THE VARIATION IN DEVELOPED POWER

PhD. Mrzljak Vedran[1], PhD. Student Eng. Poljak Igor[2], Student Jurić Antonio[1]
[1]Faculty of Engineering, University of Rijeka, Vukovarska 58, 51000 Rijeka, Croatia
[2]Department of maritime sciences, University of Zadar, Mihovila Pavlinovića 1, 23000 Zadar, Croatia

E-mail: vedran.mrzljak@riteh.hr, ipoljak2@unizd.hr, anjuric@riteh.hr

Abstract: *In this paper is presented an exergy analysis of low power steam turbine with one Curtis stage which drives the main feed water pump (MFPT) in the conventional LNG carrier steam propulsion system. It was obtained an insight into the exergy efficiency and the exergy destruction change during the variation in turbine developed power. Measurements of necessary steam operating parameters were performed in seven different turbine operating points. Increase in turbine developed power from 50 kW up to maximum power of 570 kW causes a continuous increase in turbine exergy efficiency and highest exergy efficiency was obtained at the maximum turbine power. Turbine exergy destruction is influenced by steam operating parameters, steam mass flow and turbine current power. MFPT is balanced as the most of the other steam system components – maximum exergy efficiency will be obtained at the highest turbine (steam propulsion system) load on which can be expected the majority of LNG carrier operation.*

Keywords: *EXERGY EFFICIENCY, EXERGY DESTRUCTION, POWER VARIATION, LOW POWER STEAM TURBINE, CURTIS STAGE*

1. Introduction

Today, the dominant propulsion systems on LNG carriers are steam propulsion systems [1]. Each steam propulsion system consists of many components, necessary for safe and reliable operation [2]. In the most of steam propulsion systems, main high pressure feed water pump (MFP) is traditionally driven by the low power steam turbine. In this paper was analyzed main feed water pump steam turbine (MFPT) from the aspect of exergy efficiency and exergy power losses (exergy destruction) during the variation in turbine developed power. Measurements of MFPT steam operating parameters, necessary for turbine exergy analysis, were performed on conventional LNG carrier during exploitation for seven different loads. Main characteristics of the LNG carrier in whose steam propulsion system is mounted analyzed MFPT are presented in Table 1.

Table 1. *Main characteristics of the LNG carrier*

Dead weight tonnage	84,812 DWT
Overall length	288 m
Max breadth	44 m
Design draft	9.3 m
Steam generators	2 x Mitsubishi MB-4E-KS
Propulsion turbine	Mitsubishi MS40-2 (max. power 29420 kW)
MFPT	Shinko DMG 125-3 (max. power 570 kW)

MFPT is a low power steam turbine, which consists of a single Curtis stage. Steam turbines with Curtis and other stages along with their analysis can be found in [3]. Many details of the classic and specific designs of marine steam turbines can be found in [4] and [5]. The main goal of the MFPT exergy analysis was to present change in steam turbine exergy efficiency and exergy destruction during the change in turbine developed power. At each operating point was varied turbine developed power from the lowest value of 50 kW up to the maximum power of 570 kW in steps of 20 kW. During the power variation was calculated turbine exergy efficiency and exergy destruction. The results of the analysis were presented for two turbine operating points, but presented conclusions are valid also for the entire steam turbine operating range. At each operating point steam turbine developed power variation allows detecting optimal turbine loads with the highest exergy efficiency. It was compared turbine exergy efficiency and exergy destruction from the real exploitation with achieved optimal ones.

2. MFPT exergy analysis and description of the turbine power variation

2.1. Basic equations for exergy analysis

Second law of thermodynamics defines exergy analysis [6]. The main exergy balance equation for a standard volume in steady state is [7,8]:

$$\dot{X}_{\text{heat}} - P = \sum \dot{m}_{\text{OUT}} \cdot \varepsilon_{\text{OUT}} - \sum \dot{m}_{\text{IN}} \cdot \varepsilon_{\text{IN}} + \dot{E}_{\text{ex,D}} \quad (1)$$

where the net exergy transfer by heat ($\dot{X}_{\text{heat}}$) at the temperature T is equal to [9]:

$$\dot{X}_{\text{heat}} = \sum (1 - \frac{T_0}{T}) \cdot \dot{Q} \quad (2)$$

Specific exergy was defined according to [10,11] by an equation:

$$\varepsilon = (h - h_0) - T_0 \cdot (s - s_0) \quad (3)$$

The total exergy of a flow for every fluid stream can be calculated according to [12]:

$$\dot{E}_{\text{ex}} = \dot{m} \cdot \varepsilon = \dot{m} \cdot \left[(h - h_0) - T_0 \cdot (s - s_0) \right] \quad (4)$$

Exergy efficiency is also called second law efficiency or effectiveness [13]. It can be defined as:

$$\eta_{\text{ex}} = \frac{\text{Exergy output}}{\text{Exergy input}} \quad (5)$$

2.2. Exergy efficiency and exergy destruction of MFPT

Main feed water pump steam turbine (MFPT) is directly connected to the main feed water pump (MFP), Fig. 1. The main feed water pump is used in steam system for increasing the water pressure and returning it back to the steam generators. MFPT consists of a single Curtis stage, while the whole unit (steam turbine and pump) has the following characteristics [14]:

- Pump maximum capacity: 175 m^3/h
- Pump delivery height: 818 m
- Steam turbine maximum power: 570 kW

Fig. 1 presented all important steam turbine and pump parameters necessary for exergy analysis. Those parameters, related to turbine, are steam mass flow through the turbine ($\dot{m}_{\text{MFP}}$), steam specific enthalpies and steam specific entropies at the turbine inlet and outlet. Calculation of MFPT developed power requires pump water volume flow ($\dot{V}_{\text{MFP}}$) in each observed turbine operating point, which is one of the measured operating parameters during the steam system operation.

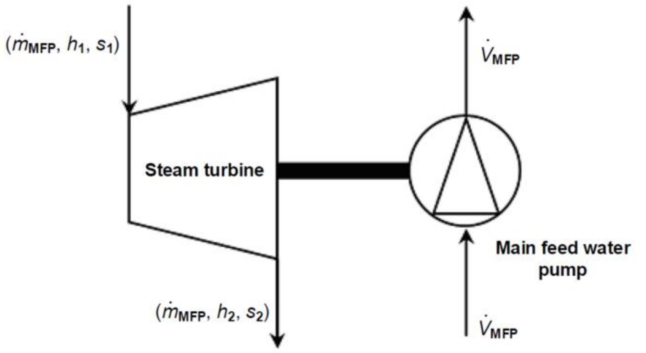

Fig. 1. *Main operating parameters at the MFPT and the main feed water pump inlet and outlet*

Developed power of MFPT was calculated from the pump water volume flow ($\dot{V}_{MFP}$) by using third degree polynomial (6), according to producer specifications [14]. Main feed water pump water volume flow in relation to the MFPT developed power was calculated for medium water density ρ_{fw} = 937.48 kg/m^3 at a water temperature of T_{fw} = 127 °C, according to producer recommendations. MFPT developed power was calculated as:

$$P_{MFPT} = 1.78582 \cdot 10^{-5} \cdot \dot{V}^3_{MFP} - 3.08892 \cdot 10^{-3} \cdot \dot{V}^2_{MFP} + \\ + 2.002 \cdot \dot{V}_{MFP} + 189.48 \quad (6)$$

where P_{MFPT} was obtained in (kW) when $\dot{V}_{MFP}$ in (m^3/h) was placed in the equation (6).

Steam mass flow through MFPT was calculated from the turbine produced power P_{MFPT}. Approximation was made according to producer specifications [14], by using third degree polynomial:

$$\dot{m}_{MFP} = -3 \cdot 10^{-5} \cdot P^3_{MFPT} + 3.1326 \cdot 10^{-2} \cdot P^2_{MFPT} - \\ 4.396794 \cdot P_{MFPT} + 2386.60 \quad (7)$$

where $\dot{m}_{MFP}$ was obtained in (kg/h) when P_{MFPT} in (kW) was placed in the equation (7).

The mass balance for the MFPT inlet and outlet is:

$$\dot{m}_{MFP,1} = \dot{m}_{MFP,2} = \dot{m}_{MFP} \quad (8)$$

According to Fig. 1 and Fig. 2, h_1 is steam specific enthalpy at the turbine inlet and h_2 is steam specific enthalpy at the turbine outlet after real (polytropic) expansion. Steam specific enthalpy at the turbine inlet (h_1) as well as steam specific entropy at the turbine inlet (s_1) was calculated from measured steam pressure and temperature at the turbine inlet. Steam specific enthalpy at the turbine outlet (h_2) was calculated from the MFPT developed power P_{MFPT} in (kW) and from steam mass flow through the turbine $\dot{m}_{MFP}$ in (kg/s) according to [9] by an equation:

$$h_2 = h_1 - \frac{P_{MFPT}}{\dot{m}_{MFP}} \quad (9)$$

The steam specific entropy at the turbine outlet (s_2) was calculated from steam specific enthalpy at the turbine outlet (h_2) and measured steam pressure at the turbine outlet (p_2).

Steam specific enthalpy at the turbine inlet (h_1) and both steam specific entropies (at the turbine inlet s_1 and outlet s_2) were calculated by using NIST REFPROP 8.0 software [15].

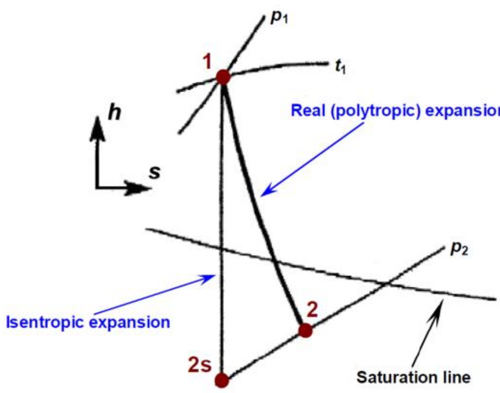

Fig. 2. *Turbine real (polytropic) and ideal (isentropic) steam expansion*

The ambient state in the LNG carrier engine room during measurements was:

- pressure: p_0 = 0.1 MPa = 1 bar,
- temperature: T_0 = 25 °C = 298.15 K.

Steam turbine exergy analysis is based on real (polytropic) steam expansion through the turbine. Based on marked turbine input and output steam flow streams, Fig. 1, MFPT exergy destruction (exergy power loss) was calculated according to [16] by using an equation:

$$\dot{E}_{MFPT,ex,D} = \dot{m}_{MFP} \cdot \varepsilon_1 - \dot{m}_{MFP} \cdot \varepsilon_2 - P_{MFPT} = \\ = \dot{m}_{MFP} \cdot (\varepsilon_1 - \varepsilon_2) - P_{MFPT} = \dot{E}_{ex,1} - \dot{E}_{ex,2} - P_{MFPT} \quad (10)$$

Specific exergies at the MFPT inlet and outlet was calculated according to equation (3) by using calculated steam specific enthalpies and steam specific entropies at the turbine inlet and outlet.

The exergy efficiency of the MFPT was calculated according to [16] by the following equation:

$$\eta_{MFPT,ex} = \frac{P_{MFPT}}{\dot{E}_{ex,1} - \dot{E}_{ex,2}} = \frac{P_{MFPT}}{\dot{m}_{MFP} \cdot [h_1 - h_2 - T_0 \cdot (s_1 - s_2)]} \quad (11)$$

2.3. The MFPT power variation description

MFPT developed power can be calculated, according to Fig. 2, by an equation:

$$P_{MFPT} = \dot{m}_{MFP} \cdot (h_1 - h_2) \quad (12)$$

Three different methods can be used for the MFPT power change. The main assumption, valid at any steam turbine operating point is always the same steam inlet pressure and temperature and the same steam outlet pressure. MFPT power change methods are:

1) Change in steam mass flow through the MFPT
2) Change in the value of steam specific enthalpy at the steam turbine outlet (h_2)
3) Combination of method 1 and 2

To present the change of MFPT exergy efficiency and exergy destruction in this paper is selected combined method (method 3) for each operating point.

Turbine developed power was varied from 50 kW up to a maximum of 570 kW in steps of 20 kW. Power change requires a change in steam mass flow through the turbine, so the adequate steam mass flow for any turbine power was calculated by using the equation (7). At each operating point, steam pressure and temperature at the turbine inlet and steam pressure at the turbine outlet remain identical to the measured data. Steam specific enthalpy at the turbine outlet (h_2) was calculated for each turbine power and steam mass flow by using equation (9). Steam specific entropy at the turbine outlet (s_2) was calculated for each turbine power and steam mass flow by using steam specific enthalpy at the turbine outlet (h_2) and measured steam pressure at the turbine outlet (p_2). Change in steam specific enthalpy at the turbine outlet (h_2), change in steam specific entropy at the turbine outlet (s_2) along with the change of steam mass flow and turbine developed power causes the change of MFPT exergy efficiency and exergy destruction which are calculated by using equations (10) and (11) in each operating point, for each described operating parameters change.

3. MFPT measurement results

Measurement results of required operating parameters at MFPT inlet and outlet along with water volume flow at the main feed water pump inlet are presented in Table 2. Operating points in Table 2 present LNG carrier steam system load (1 is the lowest system load, 7 is the highest system load). MFPT load is directly proportional to steam system load, higher steam system load denotes a higher MFPT load and vice versa. Measurement results were obtained from the existing measuring equipment mounted on the MFPT inlet and outlet and on the main feed water pump inlet.

Table 2. *MFPT and main feed water pump measurement results in various operation regimes*

Operating point	Steam pressure at the MFPT inlet (MPa)	Steam temperature at the MFPT inlet (°C)	Steam pressure at the MFPT outlet (MPa)	MFP water volume flow (m^3/h)
1	5.980	497	0.272	69.71
2	6.074	502	0.266	76.64
3	6.078	511	0.237	87.29
4	6.020	513	0.239	94.22
5	6.010	512	0.256	100.52
6	5.874	510	0.235	106.01
7	5.900	500	0.246	118.26

4. Exergy efficiency and exergy destruction change during MFPT power variation

Change in MFPT exergy efficiency and exergy destruction during the turbine developed power variation was presented in two operating points from Table 2 – operating points 1 and 4. Obtained conclusions and recommendations are also valid for the entire MFPT operating range. In every turbine operating point developed power was varied from 50 kW up to a maximum turbine power of 570 kW in steps of 20 kW.

4.1. MFPT power variation for operating point 1

MFPT exergy efficiency change in operating point 1 (Table 2), during the developed power variation is shown in Fig. 3. An increase in turbine developed power causes an increase in steam mass flow through the turbine. An increase in turbine developed power and mass flow causes a change of steam specific enthalpy at the turbine outlet (h_2) and also a change of steam specific entropy at the turbine outlet (s_2).

In operating point 1, turbine exergy efficiency continuously increases during the increase in turbine developed power because the intensity of increase in turbine developed power is higher in comparison with an increase in steam mass flow through the turbine.

At the lowest observed turbine power of 50 kW at this operating point, exergy efficiency amounts only 17.25 %, while maximum turbine exergy efficiency is obtained at the highest turbine developed power of 570 kW and amounts 69.44 %.

MFPT load is directly proportional to ship steam system load. In operating point 1, MFPT exergy efficiency during LNG carrier exploitation amounts 58.80 % what is 10.64 % lower than possible maximum exergy efficiency obtained for this operating point.

Change in MFPT exergy efficiency for operating point 1 shows that the turbine is balanced as the most of the other steam system components – maximum exergy efficiency will be obtained at the highest load on which can be expected the majority of LNG carrier operation.

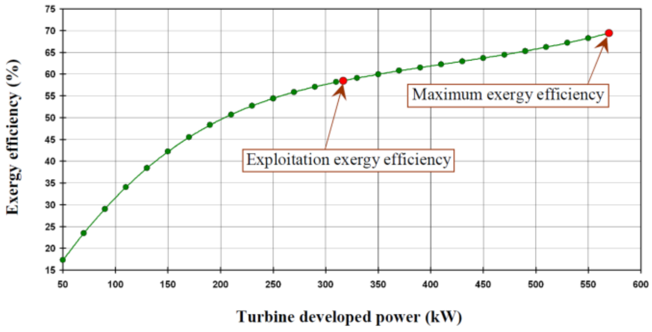

Fig. 3. *Exergy efficiency change during steam turbine power variation for operating point 1*

Fig. 4 presents the change in MFPT exergy destruction during the turbine power variation in operating point 1. At the lowest turbine power of 50 kW, exergy destruction amounts 239.81 kW. Between turbine power of 50 kW and 190 kW, exergy destruction decreases. At the turbine developed power of 190 kW was obtained the lowest exergy destruction in this operating point which amounts 203.49 kW. In the MFPT power range from 190 kW up to 510 kW exergy destruction increases. The highest exergy destruction for operating point 1 amount 260.66 kW and was obtained at turbine developed power of 510 kW. Between turbine power of 510 kW and 570 kW, exergy destruction decreases again.

During LNG carrier exploitation in operating point 1, the MFPT exergy destruction amounts 224.24 kW, while at turbine maximum exergy efficiency in this operating point (at the highest turbine developed power of 570 kW) turbine exergy destruction amounts 250.87 kW.

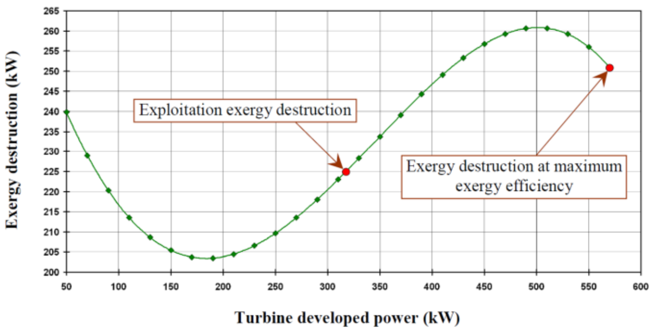

Fig. 4. *Exergy destruction change during steam turbine power variation for operating point 1*

4.2. MFPT power variation for operating point 4

MFPT exergy efficiency change in operating point 4 (Table 2), during the developed power variation is presented in Fig. 5.

In operating point 4, turbine maximum exergy efficiency is obtained as before at the highest turbine developed power and amounts 66.84 %. During LNG carrier exploitation in operating point 4, turbine exergy efficiency amounts 58.56 % what is 8.28 % lower than the maximum obtained one.

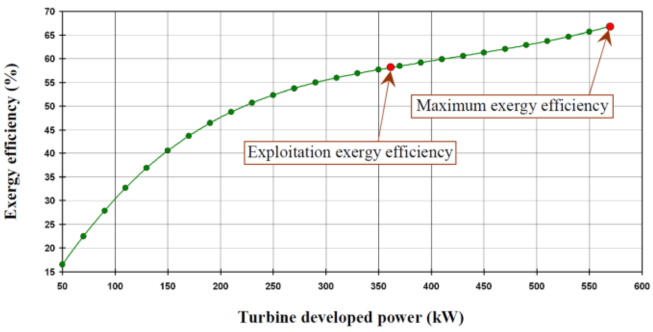

Fig. 5. *Exergy efficiency change during steam turbine power variation for operating point 4*

Fig. 6 presents the change in MFPT exergy destruction during the turbine power variation in operating point 4. At the lowest turbine power of 50 kW, exergy destruction amounts 252.37 kW. Between MFPT developed power of 50 kW and 170 kW, exergy destruction decreases and at the 170 kW was obtained the lowest exergy destruction in this operating point which amounts 218.57 kW. In the MFPT power range from 170 kW up to 510 kW exergy destruction increases and the highest exergy destruction was obtained at turbine power of 510 kW and amount 290.56 kW. Between turbine power of 510 kW and 570 kW, exergy destruction decreases again.

During LNG carrier exploitation in operating point 4, the MFPT exergy destruction amounts 258.95 kW, while at turbine maximum exergy efficiency (at the highest turbine developed power) turbine exergy destruction amounts 282.79 kW.

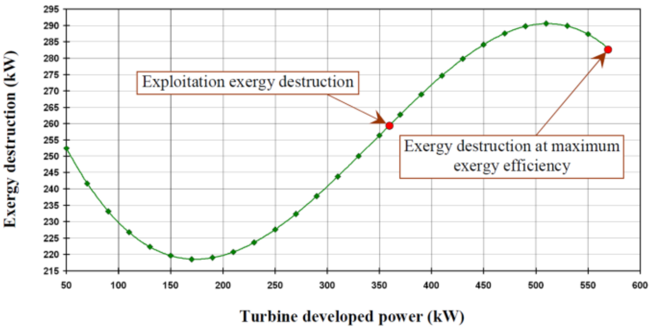

Fig. 6. *Exergy destruction change during steam turbine power variation for operating point 4*

5. Conclusions

The paper presents numerical analysis of MFPT exergy efficiency and exergy destruction change during the variation in turbine developed power.

Increase in turbine developed power from 50 kW up to 570 kW in steps of 20 kW causes a continuous increase in turbine exergy efficiency from the lowest to the highest obtained values.

The lowest MFPT exergy destruction was obtained between turbine developed power of 170 kW and 190 kW, while the highest exergy destruction was obtained for turbine developed power of 510 kW in each observed operating point. The MFPT exergy destruction is not proportional to turbine exergy efficiency, or to LNG carrier steam system load.

Analysis showed that MFPT was designed to operate at maximum exergy efficiency (obtained at turbine maximum load), as the most of the other steam propulsion system components.

NOMENCLATURE		T	temperature, °C or K
		$\dot{V}$	volume flow, m^3/h
Abbreviations:			
LNG	Liquefied Natural Gas	**Greek symbols:**	
MFP	Main feed water pump		
MFPT	Main feed water pump turbine	ε	specific exergy, kJ/kg
Latin Symbols:		η	efficiency, -
$\dot{E}$	stream flow power, kJ/s	ρ	density, kg/m^3
h	specific enthalpy, kJ/kg	**Subscripts:**	
$\dot{m}$	mass flow, kg/s or kg/h	0	ambient state
p	pressure, MPa	D	destruction
P	power, kJ/s	ex	exergy
$\dot{Q}$	heat transfer, kJ/s	IN	inlet
s	specific entropy, kJ/kg·K	OUT	outlet
$\dot{X}_{heat}$	heat exergy transfer, kJ/s	fw	feed water

6. Acknowledgment

The authors would like to extend their appreciations to the main ship-owner office for conceding measuring equipment and for all help during the exploitation measurements. This work was supported by the University of Rijeka (contract no. 13.09.1.1.05).

7. References

[1] Schinas, O., Butler, M.: *Feasibility and commercial considerations of LNG-fueled ships*, Ocean Engineering 122, p. 84–96, 2016. (doi:10.1016/j.oceaneng.2016.04.031)

[2] Fernández, I. A., Gómez, M. R., Gómez, J. R., Insua, A. A. B.: *Review of propulsion systems on LNG carriers*, Renewable and Sustainable Energy Reviews 67, p. 1395–1411, 2017. (doi:10.1016/j.rser.2016.09.095)

[3] Bloch, H. P., Singh, M. P.: *Steam turbines-Design, Applications and Re-rating*, 2nd edition, The McGraw-Hill Companies, Inc., 2009.

[4] Baldi, F., Ahlgren, F., Melino, F., Gabrielii, C., Andersson, K.: *Optimal load allocation of complex ship power plants*, Energy Conversion and Management 124, p. 344–356, 2016. (doi:10.1016/j.enconman.2016.07.009)

[5] Haglind, F.: *Variable geometry gas turbines for improving the part-load performance of marine combined cycles - Combined cycle performance*, Applied Thermal Engineering 31, p. 467-476, 2011. (doi:10.1016/j.applthermaleng.2010.09.029)

[6] Kanoğlu, M., Çengel, Y.A., Dincer, I.: *Efficiency Evaluation of Energy Systems*, Springer Briefs in Energy, Springer, 2012. (doi:10.1007/978-1-4614-2242-6)

[7] Zisopoulos, F. K., Moejes, S. N., Rossier-Miranda, F. J., Van der Goot, A. J., Boom, R. M.: *Exergetic comparison of food waste valorization in industrial bread production*, Energy 82, p. 640–649, 2015. (doi:10.1016/j.energy.2015.01.073)

[8] Nazari, N., Heidarnejad, P., Porkhial, S.: *Multi-objective optimization of a combined steam-organic Rankine cycle based on exergy and exergo-economic analysis for waste heat recovery application*, Energy Conversion and Management 127, p. 366–379, 2016. (doi:10.1016/j.enconman.2016.09.022)

[9] Ahmadi, G., Toghraie, D., Azimian, A., Ali Akbari, O.: *Evaluation of synchronous execution of full repowering and solar assisting in a 200 MW steam power plant, a case study*, Applied Thermal Engineering 112, p. 111–123, 2017. (doi:10.1016/j.applthermaleng.2016.10.083)

[10]Ahmadi, G., Toghraie, D., Ali Akbari, O.: *Solar parallel feed water heating repowering of a steam power plant: A case study in Iran*, Renewable and Sustainable Energy Reviews 77, p. 474–485, 2017. (doi:10.1016/j.rser.2017.04.019)

[11]Mrzljak, V., Poljak, I., Medica-Viola, V.: *Dual fuel consumption and efficiency of marine steam generators for the propulsion of LNG carrier*, Applied Thermal Engineering 119, p. 331–346, 2017. (doi:10.1016/j.applthermaleng.2017.03.078)

[12]Mrzljak, V., Poljak, I., Mrakovčić, T.: *Energy and exergy analysis of the turbo-generators and steam turbine for the main feed water pump drive on LNG carrier*, Energy Conversion and Management 140, p. 307–323, 2017. (doi:10.1016/j.enconman.2017.03.007)

[13]Szargut, J.: *Exergy Method - Technical and Ecological Applications*, WIT Press, 2005.

[14]*Final drawing for Main Feed Pump & Turbine*, Shinko Ind. Ltd., Hiroshima, Japan, 2006., internal ship documentation

[15]Lemmon, E.W., Huber, M.L., McLinden, M.O.: *NIST reference fluid thermodynamic and transport properties-REFPROP*, version 8.0, User's guide, Colorado, 2007.

[16]Erdem, H.H., Akkaya, A.V., Cetin, B., Dagdas, A., Sevilgen, S.H., Sahin, B., Teke, I., Gungor, C., Atas, S.: *Comparative energetic and exergetic performance analyses for coal-fired thermal power plants in Turkey*, International Journal of Thermal Sciences 48, p. 2179–2186, 2009. (doi:10.1016/j.ijthermalsci.2009.03.007)